Translational diffusion of liquids at surfaces of microporous materials: Theoretical analysis of field-cycling magnetic relaxation measurements

J.-P. Korb,[1] M. Whaley-Hodges,[2] and R. G. Bryant[2]
[1]*Laboratoire de Physique de la Matière Condensée, CNRS, Ecole Polytechnique, 91128 Palaiseau, France*
[2]*Department of Chemistry, University of Virginia, Charlottesville, Virginia 22901*
(Received 21 January 1997)

We present a theory of nuclear-spin relaxation appropriate to the case of a mobile liquid dipolar spin diffusing in a quasi-two-dimensional model porous system in the presence of rare paramagnetic impurities fixed at the surface of the pores. This theory predicts that the ^{1}H spin-lattice relaxation rate will be linear in two parts when plotted as a function of the logarithm of the magnetic-field strength and the slopes of these distinct linear regions should be in the ratio 10:3. The theory predicts also a typical pore size dependence for such a rate. The theory is tested at several temperatures using acetone, acetonitrile, dimethylformamide, and dimethylsulfoxide on microporous chromatographic glass beads that have paramagnetic ion impurities at the level of 40 ppm. ^{1}H spin-lattice relaxation rates are recorded over magnetic-field strengths corresponding to ^{1}H Larmor frequencies between 0.01 and 30 MHz using a field-switched magnetic relaxation dispersion spectrometer. The data support the theory quantitatively. The diffusion constant $D_{I\perp}$ for the proton-bearing molecule perpendicular to the normal of the pore surface is found to be nearly a factor of 10 smaller than in the bulk solvents. It is characterized by a small activation energy similar to those in the bulk solvent. These results demonstrate that magnetic relaxation dispersion at low magnetic-field strengths in high-surface-area heterogeneous systems may be quantitatively understood in terms of the parameters of the spatial confinement and the local translational dynamics. [S1063-651X(97)07808-2]

PACS number(s): 47.55.Mh, 68.45.Gd, 76.60.Es

I. INTRODUCTION

Nuclear-magnetic-relaxation methods offer a variety of opportunities for characterizing the molecular dynamics in confined environments [1–7]. Systems of interest are high-surface-area materials including biological tissues, chromatographic supports, heterogeneous catalytic materials, and natural microporous materials such as clay minerals and rocks.

The magnetic-field dependence of the nuclear-spin relaxation rate is a rich source of dynamical information [8–10]. Varying the magnetic field changes the Larmor frequency and thus the fluctuations to which the nuclear-spin relaxation is sensitive. Moreover, this method permits a more complete characterization of the dynamics than the usual measurements as a function of temperature at fixed magnetic-field strength because many common solvent liquids have phase transitions that may alter significantly the character of the dynamics over the temperature range usually studied. Further, the magnetic-field dependence of the spin-lattice relaxation rate $1/T_1$ provides a good test of the theories that relate the measurement to the microdynamical behavior of the liquid. This is especially true in spatially confined systems where the effects of reduced dimensionality may force more frequent reencounters of spin-bearing molecules that may alter the correlation functions that enter the relaxation equations in a fundamental way.

We may distinguish two classes of high-surface-area systems: solid phases that are proton rich such as biological macromolecules including proteins, carbohydrates, and engineering polymers such as polystyrene and solid phases that are proton poor such as microporous glasses, zeolites, or the clay minerals. In the first class, cross relaxation between the protons of the liquid and those of the solid may make dominant contributions to the nature of the magnetic-field dependence of the nuclear-spin relaxation rate observed [9]. In a number of such proton-rich cases studied, the magnetic-field dependence of the liquid spin-relaxation reports the magnetic-field dependence of the solid-phase relaxation. In the second case of the proton-poor solid, other effects dominate the liquid spin relaxation including, in particular, those that are dependent on the translational diffusion of liquid in the neighborhood of solid surfaces [4,5].

In the present study, we are interested in high-surface-area materials such as microporous chromatographic glass that contains contaminant concentrations of paramagnetic centers (iron) that may alter the nature of the relaxation significantly. In particular, the paramagnetic centers provide a large magnetic moment and local dipolar field in which the diffusing liquid spins move. The effects of the electron magnetic moments are large and dominate unambiguously the proton spin-lattice relaxation at low magnetic-field strengths.

In this paper we present the magnetic-field dependence of the proton spin-lattice relaxation of four polar but aprotic solvents in suspension of controlled pore chromatographic glass beads. The observed magnetic-field dependence of the proton spin-lattice relaxation rate is unique in that it is well represented by two linear regions when the relaxation rate is plotted against the logarithm of the Larmor frequency. This observation, over four orders of magnitude of the magnetic field, is quantitatively consistent with the theory we develop here that treats the mobile liquid spins diffusing in a surface restricted geometry and in the presence of the fixed magnetic dipolar fields of trace paramagnetic impurities on the glass surface. Our method provides a direct measurement of the

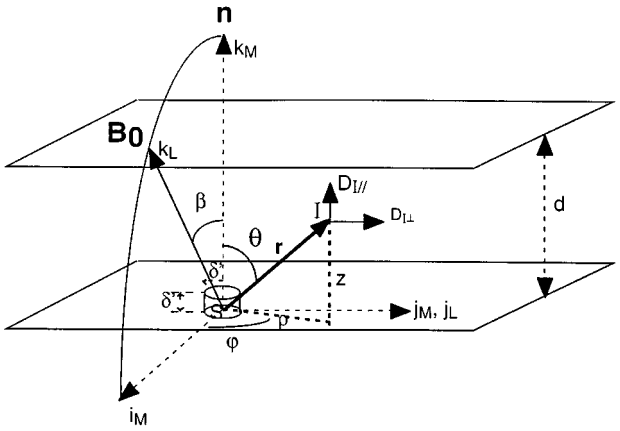

FIG. 1. Schematic diagram of the slit or channel pore model. The nuclear spin I diffuses in an infinite layer of thickness d between two flat solid surfaces in the dipolar field of a very small quantity of paramagnetic spins S fixed on the surface. The surface density σ_s of the S-spin-bearing molecules is sufficiently small that the distance between two spins S at the surface $1/\sqrt{\sigma_s}$ is of the order of or larger than d. The M axes are fixed in the layered system. The L axes are fixed in the laboratory frame, with the constant magnetic field $\mathbf{B}_0$ at the angle β from the normal axis $\mathbf{n}$. The relative cylindrical polar coordinates ρ, φ, and z are based on the M frame. The smallest value of ρ and z corresponding to the distance of minimal approach of the two I- and S-spin-bearing molecules at surface is δ'. The distinction between the translational diffusion constants of spin I are indicated on the diagram.

translational diffusion of polar liquids in close proximity to the paramagnetic centers at the pore surface.

II. THEORY OF HETERONUCLEAR DIPOLAR RELAXATION BY TRANSLATIONAL DIFFUSION OF FLUIDS IN A MODEL POROUS SYSTEM

We consider an ensemble of a large number of nuclear spins $I=\frac{1}{2}$ (protons) in a given fluid of uniform density that diffuse within an infinite layer of finite thickness d between two flat solid surfaces in the presence of a constant magnetic field $\mathbf{B}_0$ oriented at the angle β from the normal axis $\mathbf{n}$ (Fig. 1). We consider also the presence of a very small quantity of fixed paramagnetic species of spins S uniformly distributed on these surfaces with a surface density σ_s. We restrict our calculation to the case of highly diluted paramagnetic species where the average distance between two S spins on the surface $1/\sqrt{\sigma_s}$ is about or even larger than the pore size d (Fig. 1). This layered geometry simulates the simplest type of pore, the slit or channel pore, which is sufficient to account for the quasi-two-dimensional characteristics implied by the observed logarithmic magnetic-field dependence of the proton spin-lattice relaxation rates in the calibrated porous glass beads (see Sec. IV).

Because the magnetic moment of the paramagnetic species is large ($\gamma_S=658.21\gamma_I$), there is no ambiguity about the relaxation mechanism of the diffusing proton spins I, which is the intermolecular dipolar relaxation process induced by fixed spins S and modulated by the translational diffusion of the mobile spins I in close proximity to these surfaces. Basically, the nuclear spin-lattice relaxation rate of the diffusing spins I is given formally by the general expression $1/T_{1I}$ [11],

$$\frac{1}{T_{1I}}=\frac{2}{3}(\gamma_I\gamma_S\hbar)^2S(S+1)\left[\frac{1}{3}J_L^{(0)}(\omega_I-\omega_S)+J_L^{(1)}(\omega_I)+2J_L^{(2)}(\omega_I+\omega_S)\right], \tag{1}$$

where the spectral density $J_L^{(m)}$ in the laboratory frame (L) of the basis $\mathbf{i}_L,\mathbf{j}_L,\mathbf{k}_L\|\mathbf{B}_0$ (Fig. 1) is the exponential Fourier transform

$$J_L^{(m)}(\omega)=\int_{-\infty}^{\infty}G_L^{(m)}(\tau)e^{i\omega\tau}d\tau \tag{2a}$$

of the stationary pairwise dipolar correlation function $G_L^{(m)}(\tau)$ $\{m\in(-2,+2)\}$ given by

$$G_L^{(m)}(\tau)=\langle F_L^{(-m)}(t)F_L^{(-m)*}(t+\tau)\rangle. \tag{2b}$$

Equation (2b) describes the persistence of the second-order irreducible spherical spatial dipolar tensor $F_L^{(m)}(t)$ between the magnetic moments associated with the spins I and S and modulated by the translational diffusion of spins I relative to the fixed spins S during a short time interval τ [11]. The notation $\langle\,\rangle$ stands for the ensemble average over all the positions of the spins I at times 0 and τ for a given density σ_S/d of spins S.

According to the dynamical model described in Fig. 1, it is much simpler to calculate the time dependences of the dipolar correlations in the lamellar frame M of the basis $\mathbf{i}_M,\mathbf{j}_M,\mathbf{k}_M\|\mathbf{n}$. For that we use the well-known properties of the Wigner D functions [12] to express $F_L^{(m)}(t)$ as it comes through a succession of three coordinate rotations $\mathcal{P}\rightarrow M\rightarrow L$,

$$\begin{aligned}F_L^{(-m)}(t)&=\sum_{m'=-2}^{+2}F_M^{(-m')}(t)D^{(2)*}_{-m,m'}(\alpha=0,\beta,\gamma=0)\\&=\sum_{m'=-2}^{+2}\left(\sum_{m''=-2}^{+2}F_{\mathcal{P}}^{(-m'')}(t)\,\delta_{m'',0}D^{(2)*}_{m',m''}(\varphi,\theta,0)\right)D^{(2)*}_{-m,m'}(\alpha=0,\beta,\gamma=0)\\&=\sqrt{\frac{6\pi\rho'}{5}}\frac{1}{r^3(t)}\sum_{m'=-2}^{2}Y_2^{(m')}(\theta(t),\varphi(t))d^{(2)}_{-m,m'}(\beta).\end{aligned} \tag{3}$$

In Eq. (3), α,β,γ are the Eulerian angles that rotate the L basis into the M basis. Because of cylindrical symmetry around **n**, we have chosen these angles as $\alpha=\gamma=0$; thus $D^{(2)}_{mm'}(\alpha=0,\beta,\gamma=0)=d^{(2)}_{mm'}(\beta)$ (Wigner rotation coefficients) [12]. The principal axis frame $\mathcal{P}$ ($\mathcal{P}$AF) has its **z** axis along the interspin I-S vector **r** and the Kronecker symbol $\delta_{m''0}$ shows the restriction of the dipolar tensor to the axial values $F^{(0)}_{\mathcal{P}}(t)=\sqrt{\frac{3}{2}}/r^3$ and $F^{(\pm 1)}_{\mathcal{P}}(t)=F^{(\pm 2)}_{\mathcal{P}}(t)=0$. The angles $(\varphi,\theta,0)$ are the angles that rotate the M basis into the PAF basis and $Y^{(m')}_2$ represent the second-order spherical harmonics. In order to facilitate the calculation of Eq. (2b), we use the cylindrical coordinates for the time-dependent spatial variables (ρ,z,φ) and express $F^{(m)}_L(t)$ as

$$F^{(-m)}_L(t)=\sum_{m'=-2}^{+2} f^{(m')}_2(t)e^{im'\varphi}d^{(2)}_{-m,m'}(\beta), \tag{4a}$$

with

$$f^{(0)}_2(t)=\frac{1}{2}\sqrt{\frac{3}{2}}\frac{2z^2-\rho^2}{(z^2+\rho^2)^{5/2}},$$

$$f^{(\pm 1)}_2(t)=\mp\frac{3}{2}\frac{\rho z}{(z^2+\rho^2)^{5/2}}, \tag{4b}$$

$$f^{(\pm 2)}_2(t)=\frac{3}{4}\frac{\rho^2}{(z^2+\rho^2)^{5/2}}.$$

Here all the $f^{(m)}_2$ are real functions. Substituting Eq. (4a) into Eq. (2b) gives the ensemble average for the dipolar correlation functions in the laboratory frame L,

$$G^{(m)}_L(\tau)=\sum_{m'=-2}^{+2}\sum_{m''=-2}^{+2} d^{(2)}_{-m,m'}(\beta)d^{(2)}_{-m,m''}(\beta) \times\langle f^{(m')}_2(\rho_0,z_0)f^{(m'')}_2(\rho,z)e^{i[m'\varphi_0-m''\varphi]}\rangle. \tag{5}$$

This average will be replaced by their usual integral average over the normalized conditional probability $P(\rho,\varphi,z,\tau|\rho_0,\varphi_0,z_0,\tau=0)$ that ρ,φ in $(\mathbf{i}_M,\mathbf{j}_M)$ and $z(\|\mathbf{k}_M)$ take their values at time τ, given their values ρ_0, φ_0, and z_0, at time $\tau=0$,

$$\begin{aligned}G^{(m)}_L(\tau)=&\sum_{m'=-2}^{+2}\sum_{m''=-2}^{+2} d^{(2)}_{-m,m'}(\beta)d^{(2)}_{-m,m''}(\beta)\\ &\times\int_0^{2\pi}d\varphi_0\int_{C_{M\rho}}d^2\rho_0\int_{C_{Mz}}dz_0 p(0)f^{(m')}_2(\rho_0,z_0)\\ &\times e^{i[m'\varphi_0]}\int_0^{2\pi}d\varphi\int_{C_{M\rho}}d^2\rho\int_{C_{Mz}}\\ &\times dz\ P(\rho,\varphi,z,\tau|\rho_0,\varphi_0,z_0,\tau=0)f^{(m'')}_2(\rho,z)\\ &\times e^{-i[m''\varphi]}.\end{aligned} \tag{6}$$

Here $C_{M\rho}$ and C_{Mz} correspond to the ρ and z domains of integration in the lamellar frame M (Fig. 1) and $p(0)=\sigma_S/d$ represents the uniform density of spins pairs I-S at equilibrium.

When considering translational diffusion of the I-spin-bearing molecules in this quasi-two-dimensional geometry, we have shown [4] that the anisotropy of the dynamics is described by an unbounded diffusion perpendicular to the normal axis **n** and a bounded diffusion parallel to this axis. According to this diffusion model, P is defined as a product of a bounded $P_\parallel$ and unbounded $P_\perp$ terms

$$P(\vec{\rho},z,\tau|\vec{\rho}_0,z_0,\tau=0)=P_\perp(\vec{\rho},\tau|\vec{\rho}_0,\tau=0)P_\parallel(z,\tau|z_0,\tau=0), \tag{7}$$

which individually verify the initial conditions

$$P_\perp(\tau=0)=\delta(\vec{\rho}-\vec{\rho}_0),\quad P_\parallel(\tau=0)=\delta(z-z_0) \tag{8}$$

and boundary conditions of zero flux in the **n** direction at the limits of the layer of thickness d,

$$\frac{\partial}{\partial z}P_\parallel(z=0,\tau)=\frac{\partial}{\partial z}P_\parallel(z=d,\tau)=0. \tag{9}$$

$P_\parallel$ is obtained by using the well-known procedures for solving the diffusion equation [13] and the assumed unbounded Gaussian conditional probability $P_\perp$ is expressed by its Fourier transform in the reciprocal k space where we used the Jacobi-Anger expansion of $\exp(i\mathbf{k}\cdot\boldsymbol{\rho})$ in terms of the integer Bessel function $J_m(k\rho)$ of integer order m:

$$P_\perp(\vec{\rho},\tau|\vec{\rho}_0,\tau=0)=\frac{1}{2\pi}\sum_{m=-\infty}^{+\infty}\int_0^\infty dk\ k\ \exp(-k^2D_{I\perp}\tau) \times J_m(k\rho)J_m(k\rho_0)\exp[im(\varphi_0-\varphi)], \tag{10a}$$

$$P_\parallel(z,\tau|z_0,\tau=0)=\frac{1}{d}\left[1+2\sum_{I=1}^{\infty}\exp\left(-\frac{l^2D_{I\parallel}\tau}{d^2}\right) \times\cos\left(\frac{l\pi z}{d}\right)\cos\left(\frac{l\pi z_0}{d}\right)\right]. \tag{10b}$$

In Eqs. (10a) and (10b), $D_{I\parallel}$ and $D_{I\perp}$ are the translational diffusion coefficients of spin I in directions parallel and perpendicular to **n**, respectively. Because the electron spins are fixed, $D_{S\perp}=D_{S\parallel}=0$.

Substituting Eqs. (10a) and (10b) into Eq. (6) transforms $G^{(m)}_L(\tau)$ as a superposition of transverse and parallel pairwise dipolar correlation functions $G^{(m)}_L(\tau)=G^{(m)}_{L\perp}(\tau)+G^{(m)}_{L\parallel}(\tau)$. However, it will be seen in the following that only time scales much longer than either of the diffusional correlation times $\tau_\perp$ or $\tau_\parallel$ contribute significantly to the low-field spin-lattice relaxation rate. This approximation allows an immediate simplification of the overall conditional probability P, which comes from the different time dependences of the bounded $P_\parallel$ and unbounded $P_\perp$ terms. Equation (10b) shows that the back and forth molecular motion along the z direction causes $P_\parallel$ to approach rapidly its equilibrium value $1/d$. In consequence, $G^{(m)}_{L\parallel}(\tau)$ tends to zero for time τ much larger than the longest parallel correlation time $\tau_\parallel=d^2/D_{I\parallel}$.

Contrarily, the presence of a simple Gaussian term $\exp(-k^2 D_{I\perp}\tau)$, in Eq. (10a) shows that only the long-wavelength transverse diffusing modes ($k\to 0$) dominate $G_{L\perp}^{(m)}(\tau)$ for time τ much larger than the transverse diffusional correlation time $\tau_\perp = \delta^2/(4D_{I\perp})$. Such a latter time is necessary to make a single random molecular jump, of the order of the molecular size δ, parallel to the pore surface. In consequence, the overall conditional probability P is described at long times by

$$P(\rho,\varphi,z,\tau|\rho_0,\varphi_0,z_0,\tau=0)\approx \frac{1}{2\pi d}\sum_{m=-\infty}^{+\infty}\int_0^\infty dk\ k \times\exp(-k^2 D_{I\perp}\tau)J_m(k\rho) \times J_m(k\rho_0)\exp[im(\varphi_0-\varphi)]. \tag{11}$$

After substitution of Eq. (11) into Eq. (6), integration over the angles φ and φ_0, and application of some symmetry relations, one has

$$G_L^{(m)}(\tau)=\sum_{m'=-2}^{+2}|d^{(2)}_{-m,m'}(\beta)|^2 G_M^{(m')}(\tau), \tag{12}$$

where the $G_M^{(m')}(\tau)$ $\{m'\in(-2,+2)\}$ are the pairwise dipolar correlation functions in the lamellar frame M, given by

$$G_M^{(m')}(\tau)=\frac{2\pi\sigma_s}{d^2}\int_0^\infty dk\ k\ \exp(-k^2 D_{I\perp}\tau) \times\left|\int_{C_{Mz}}dz\int_{C_{M\rho}}d\rho\ \rho\ f_2^{(m')}(\rho,z)J_{m'}(k\rho)\right|^2. \tag{13}$$

It is known that for a polar liquid in contact with a solid surface, there are two distinct phases in fast exchange: a surface-affected liquid phase of thickness about a molecular diameter δ and a bulk liquid phase. Our earlier NMR studies [4,5,7] proved the applicability of this biphasic fast exchange model. In the following we introduce the distance of minimal approach δ' between spins I and S at the pore surface (Fig. 1). Typically, δ' is comparable to the radius of the molecules $\delta/2$. A typical choice is $\delta'=\delta/2n$, with n being a parameter of the order of unity. This parameter takes into account a variable distance of minimal approach at the surface between the spin-bearing molecules and does not affect the essential features of our results. In consequence, we separate the integral calculations of Eq. (13) into bulk and surface contributions (see Appendix A)

$$G_M^{(m')}(\tau)=G_{M,\text{bulk}}^{(m')}(\tau)+G_{M,\text{surface}}^{(m')}(\tau). \tag{14}$$

In the first region, the spin I is restricted to the bulk part of the pore and the C_{Mz} and $C_{M\rho}$ are $\delta'\leq z\leq d-\delta'$ and $0\leq\rho<\infty$, respectively. In the second region, the spin I is restricted to the two surface layers of the pore and the C_{Mz} and $C_{M\rho}$ are $0\leq z\leq\delta'$ and $\delta'\leq\rho<\infty$, respectively. We then exclude from the integrations a very small cylindrical volume of size δ'^3 around the highly diluted spin species S on the pore surface. As we are interested only in the nuclear relaxation rates at low field strengths, the real boundary condition in close proximity to such an excluded volume does not affect the validity of Eq. (10a) because its effects should appear at high magnetic field [14].

After calculations detailed in Appendix A and provided that $d\gg\delta'$, one finds that at long times ($\tau\gg\tau_\perp$), the surface contribution dominates the correlations for $G_M^{(0)}(\tau)$, while the bulk contribution dominates the correlations for $G_M^{(1)}(\tau)$ and $G_M^{(2)}(\tau)$:

$$G_M^{(0)}(\tau)\approx\frac{3}{8}\frac{\pi\sigma_s}{d^2\delta'^2}\left(\frac{\tau_\perp}{\tau}\right),$$
$$G_M^{(1)}(\tau)\approx\frac{1}{4}\frac{\pi\sigma_s}{\delta'^4}\left(\frac{\tau_\perp}{\tau}\right)^2, \tag{15}$$
$$G_M^{(2)}(\tau)\approx\frac{1}{16}\frac{\pi\sigma_s}{\delta'^4}\left(\frac{\tau_\perp}{\tau}\right)^2.$$

The different power laws present in Eq. (15) show indeed that the persistence of the pairwise dipolar correlations at long times is dominated by $G_M^{(0)}(\tau)$. Physically, its slow time decay (proportional to $1/\tau$) comes from the permanent back and forth motion of the moving spins, I, parallel to the pore walls, in close proximity to the fixed spin S. Such a quasi-two-dimensional diffusive motion maintains the dipolar correlations during a much longer time than in the bulk [15]. How far from each S spin does this two dimensionality extend? A typical distance might be of the order of $1/\sqrt{\sigma_s}$ between two paramagnetic spins S at the pore surface. We will see in Sec. IV that such a distance is about 170 Å, which is sufficiently large to validate the assumption of highly diluted paramagnetic spin species in the calculation of the pairwise surface dipolar correlation functions between the moving spins I and a single spin S. Such a limitation has not been used in the derivation of the surface correlation function, which considers an unbounded diffusion along the pore wall. However, this distance is sufficiently large in comparison to the effective range of dipolar interactions between spins I and S that it does not affect the results presented in Eqs. (15).

Similarly, we perform in Appendix B analytic calculations of the Fourier transforms of Eq. (13) for the overall spectral densities $J_M^{(m')}(\omega)=J_{M,\text{bulk}}^{(m')}(\omega)+J_{M,\text{surface}}^{(m')}(\omega)$ when $\omega\tau_\perp\ll 1$ and $d\gg\delta'$. Numerical calculations of Eqs. (B6), (B9), and (B10a)–(B10d) for $d/\delta'\sim 25$ or 50 and in the range $5\times10^{-5}\leq\omega\tau_\perp\leq 0.1$ show that the expression of $J_M^{(0)}(\omega)$

$$J_M^{(0)}(\omega)=\frac{3\pi\sigma_s\tau_\perp}{2d^2\delta'^2}\left[\ln\left(\frac{d}{\delta'}+1\right)-3.078+\frac{1}{4}\ln\left(1+\frac{1}{\omega^2\tau_\perp^2}\right)+O(\sqrt{\omega\tau_\perp})\right] \tag{16}$$

dominates largely $J_M^{(1)}(\omega)$ and $J_M^{(2)}(\omega)$ at low frequency. The logarithmic divergence of the dominant term of the spectral density at low frequency constitutes the essential conclusion of this theoretical part. This unique dependence on the

magnetic-field strength or Larmor frequency is favored by the quasi-two-dimensionality in close proximity to the paramagnetic impurity, which enhances drastically the frequency of reencounters between the I- and S-spin-bearing molecules [15].

Now we substitute these calculated spectral densities in Eq. (12) adapted for the spectral density in the laboratory frame. Finally, we make a powder average over the angle β labeled as $\langle\ \rangle$ in order to take into account the random orientation of the local lamellar axis $\mathbf{n}$ relative to the constant direction of the static magnetic field $\mathbf{B}_0$,

$$\langle J_L^{(0)}(\omega)\rangle = \left\langle \sum_{m'=-2}^{+2} \left| d_{0,m'}^{(2)}(\beta) \right|^2 J_M^{(m')}(\omega) \right\rangle$$
$$= \tfrac{1}{5}[J_M^{(0)}(\omega) + 2J_M^{(1)}(\omega) + 2J_M^{(2)}(\omega)] \approx \tfrac{1}{5} J_M^{(0)}(\omega),$$
$$\langle J_L^{(1)}(\omega)\rangle = \left\langle \sum_{m'=-2}^{+2} \left| d_{1,m'}^{(2)}(\beta) \right|^2 J_M^{(m')}(\omega) \right\rangle \approx \tfrac{1}{5} J_M^{(0)}(\omega), \tag{17}$$
$$\langle J_L^{(2)}(\omega)\rangle = \left\langle \sum_{m'=-2}^{+2} \left| d_{2,m'}^{(2)}(\beta) \right|^2 J_M^{(m')}(\omega) \right\rangle \approx \tfrac{1}{5} J_M^{(0)}(\omega).$$

From a theoretical point of view these expressions, as well as Eqs. (18) and (19), imply that there is no observable deviation from an exponential decay of the calculated overall magnetization. We have discussed in detail in Appendix C the validity of such an approximation. From the experimental point of view and to within our precision ($\sim 3\%$), the observed relaxation decays are exponential. Our ability to detect a rapid nonexponential component is poor because of the finite magnetic-field switching times, which add up to tens of milliseconds. The last step of the calculation consists in substituting Eq. (17) into the powder average of Eq. (1), which yields

$$\left\langle \frac{1}{T_{1I}} \right\rangle = \frac{\pi}{15} \sigma_S (\gamma_I \gamma_S \hbar)^2 S(S+1) \frac{\tau_\perp}{d^2 \delta'^2} \left[10 \ln\left(\frac{d}{\delta'} + 1 \right) \right.$$
$$- 30.8 + \tfrac{1}{4}\{\ln[1 + (\omega_I - \omega_S)^{-2} \tau_\perp^{-2}]$$
$$\left. + 3 \ln(1 + \omega_I^{-2} \tau_\perp^{-2}) + 6 \ln[1 + (\omega_I + \omega_S)^{-2} \tau_\perp^{-2}]\} \right]. \tag{18}$$

A simplification occurs in Eq. (18) because of the relation $\omega_S = 658.21 \omega_I$, which gives finally the theoretical expression for the proton spin-lattice relaxation rate $1/T_{1I}$, valid at low frequency for the model considered

$$\frac{1}{T_{1I}} = \frac{\pi}{15} \sigma_S (\gamma_I \gamma_S \hbar)^2 S(S+1) \frac{\tau_\perp}{d^2 \delta'^2} \left[10 \ln\left(\frac{d}{\delta'} + 1 \right) - 30.8 \right.$$
$$\left. + \frac{1}{4} [7 \ln(1 + \omega_S^{-2} \tau_\perp^{-2}) + 3 \ln(1 + \omega_I^{-2} \tau_\perp^{-2})] \right], \tag{19}$$

where we have omitted the notation $\langle\ \rangle$.

The bilogarithmic magnetic-field dependence obtained (Fig. 2) permits the verification of the uniqueness of the present anisotropic and quasi-two-dimensional diffusion model. Such an analytical expression identifies clearly the influence of both the diffusion constant $D_{1\perp}$ and the pore size d on the frequency dependence of $1/T_{1I}$. We note that the ratio of 10:3 between the slopes of the linear portions of these semilogarithmic plots (Fig. 2) results from the usual coefficients of the required spectral densities in the basic nuclear paramagnetic relaxation equation [16]. This factor agrees with the observed data of Figs. 3 and 4. In the next section we apply the unique properties of the magnetic-field dependences of $1/T_{1I}$ to probe the microdynamics of different polar solvents at the surfaces of calibrated microporous glass systems.

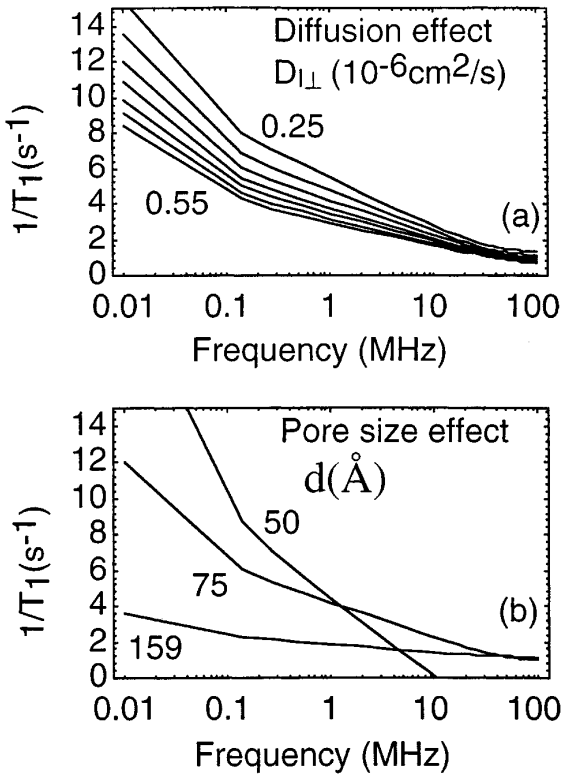

FIG. 2. Calculated variations of the magnetic-field dependences of proton spin-lattice relaxation rates given by Eq. (19) (a) for pore size $d = 75$ Å, molecular size $\delta = 7$ Å, $\delta' = 4.1$ Å, and different values of the diffusion coefficient $D_{I\perp}$: (from top to bottom) 0.25×10^{-6} cm^2/s (0.30, 0.35, 0.40, 0.45, 0.50) and 0.55×10^{-6} cm^2/s and (b) for $D_{I\perp} = 0.35 \times 10^{-6}$ cm^2/s, $\delta = 7$ Å, $\delta' = 4.1$ Å, and varying the pore size d (Å) as shown.

III. EXPERIMENT

Proton nuclear magnetic relaxation rates were measured using an instrument of the Redfield design [17] constructed partly in a collaboration with Brown and Koenig of the IBM Watson Laboratory, which is described elsewhere [18,19]. This instrument switches current in a copper solenoid that is immersed in liquid nitrogen. Spins are polarized in a field corresponding to a ^{1}H Larmor frequency of 30 MHz and then the field is switched to a field of interest for a variable relaxation period after which the field is switched to a ^{1}H Larmor frequency of 7.25 MHz, where the magnetization is detected by a Hahn spin echo. This field-switching technique

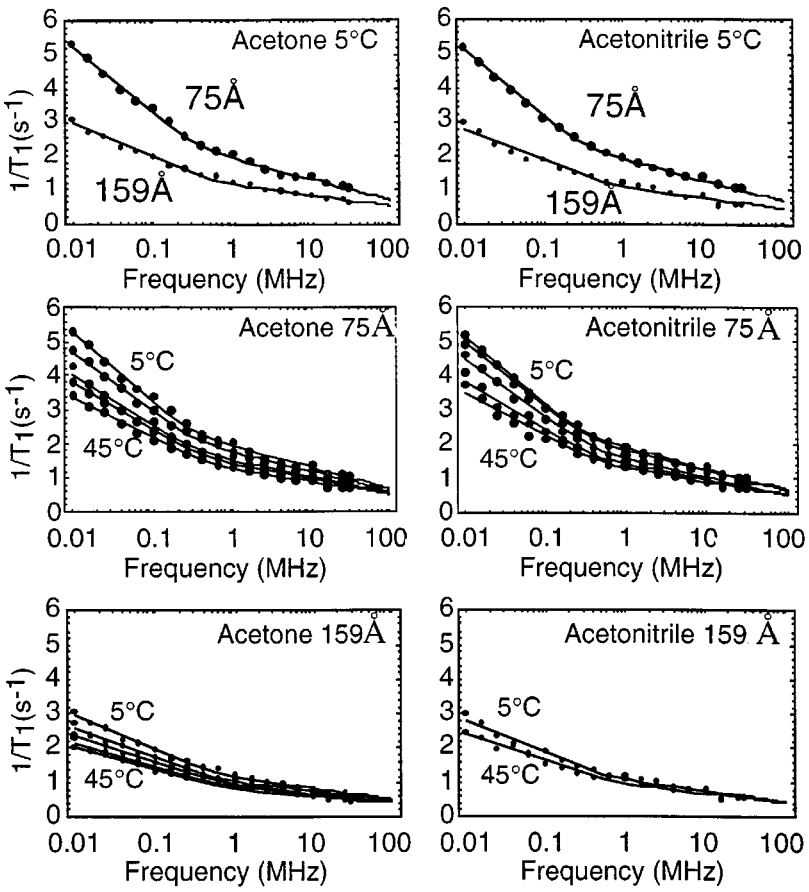

FIG. 3. Magnetic-field dependences of ^{1}H spin-lattice relaxation rates of acetone and acetonitrile embedded in a packed samples of calibrated porous glasses beads at (from top to bottom) 5 °C, 15 °C, 25 °C, 35 °C, and 45 °C. The large and small experimental black points correspond to glasses of pore sizes 75 and 159 Å, respectively. The continuous lines correspond to the best fits to Eq. (19) as discussed in the text. The field strength is shown as the ^{1}H Larmor frequency.

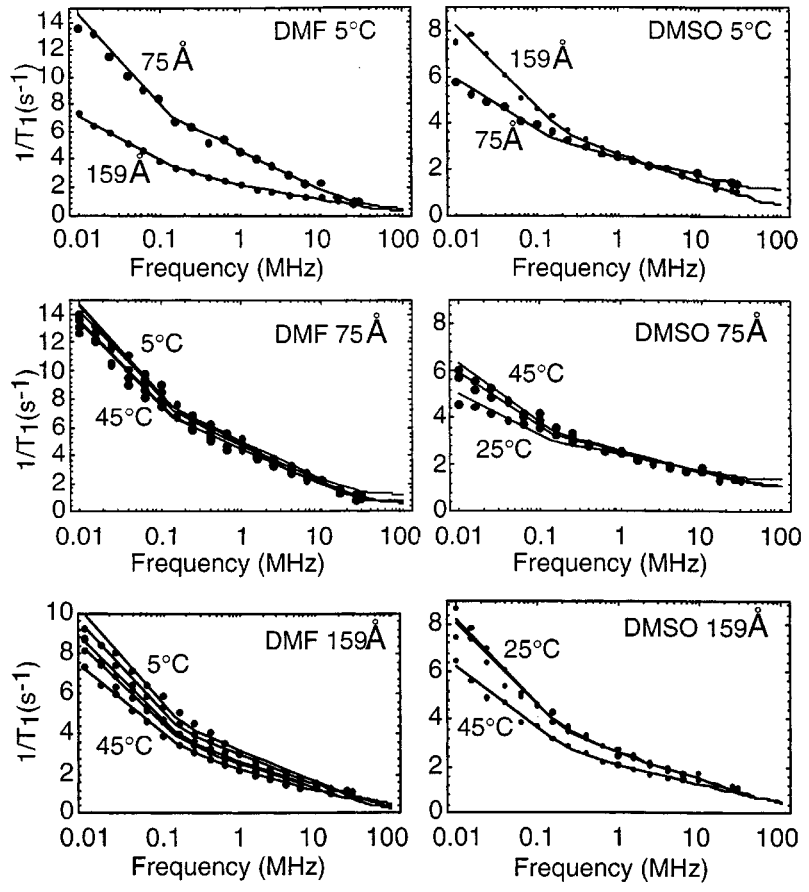

FIG. 4. Magnetic-field dependences of ^{1}H spin-lattice relaxation rates of DMF and DMSO embedded in packed samples of calibrated porous glasses beads at (from top to bottom) 5 °C, 15 °C, 25 °C, 35 °C, and 45 °C. The large and small experimental black points correspond to glasses of pore sizes 75 and 159 Å, respectively. The continuous lines correspond to the best fits of Eq. (19) as discussed in the text. The field strength is shown as the ^{1}H Larmor frequency.

TABLE I. Relaxation parameters.

Porous systems / Liquid	$d=75$ Å, $\sigma_s=3.46\times10^{11}$ Fe/cm^2			$d=159$ Å, $\sigma_s=4.27\times10^{11}$ Fe/cm^2	
	δ (Å)	δ' (Å)	$D_{I\perp}$[a] (10^{-5} cm^2/s)	δ' (Å)	$D_{I\perp}$[a] (10^{-5} cm^2/s)
acetone	6.1	3.7	0.14	2.1	0.25
acetonitrile	6.2	3.6	0.16	2.0	0.25[b]
DMF	7.5	4.4	0.03	2.0	0.08
DMSO	7.1	6.0	0.04	1.9	0.09

[a]Obtained at 25 °C using Eq. (19) and the other parameters in the table.
[b]Obtained at 15 °C using Eq. (19) and the other parameters in the table.

permits measurement of spin-lattice relaxation rates from 0.01 to 30 MHz with nearly constant signal-to-noise ratios. Samples are contained in 10-mm Pyrex tubes closed with both a rubber stopper and a screw cap. Temperature was controlled by a Neslab RTE-8 system using perchloroethylene as the cryogeneic fluid.

Controlled pore chromatographic glass was purchased from Sigma Chemical Company with mean pore diameters of 75 and 159 Å and specific areas of 140 and 90.9 m^2/g, respectively. Reagent grade acetone, acetonitrile, *N*,*N*-dimethylformamide (DMF) and dimethylsulfoxide (DMSO) were obtained from Mallinkrodt Chemical and J. T. Baker Chemical companies and were used without further purification. Samples were prepared gravimetrically by depositing a known mass of glass beads in a 10-mm Pyrex glass sample tube, fitted with a screw cap, then filled with the solvent of interest, and the tube shaken vigorously. The glass beads were permitted to settle, excess solvent removed by pipet, and the total mass recorded. Sample tubes were finally doubly sealed with rubber stoppers and a screw cap.

IV. RESULTS AND COMPARISON WITH THEORY

The magnetic-field dependence of the proton spin-lattice relaxation rates for suspensions of 75- and 159-Å chromatographic glass beads are reported for fields corresponding to ^{1}H Larmor frequencies from 0.01 to 30 MHz over a range of temperature from 5 °C to 45 °C for acetone and acetonitrile (Fig. 3) and for dimethylformamide and dimethylsulfoxide (Fig. 4). A common feature of these data is that the relaxation rate is linear in the logarithm of the Larmor frequency in two regions of the magnetic-field strength. This magnetic-field dependence is unusual and not predicted by commonly used theories for molecular motion in liquids. The effect of molecular confinement may alter the magnetic-field dependence of the relaxation rates significantly and produce a relaxation rate that is linear in the logarithm of the magnetic-field strength because of the correlation imposed by the boundaries on the proton-proton dipole-dipole correlations [15]. However, the effects that derive from purely nuclear-nuclear interactions are too small to account for the relaxation rates observed in these samples. The relaxation must derive from stronger interactions that may be provided by trace paramagnetic centers in the glass preparations. The iron content of these samples, checked by electron paramagnetic resonance and analytical chemistry measurements, is 45 and 36 ppm for the 75- and 159-Å pore glasses, respectively. This is sufficient to provide a dominant relaxation path for the proton spins at low magnetic-field strengths. From the specific area of the glass and if we assume that all the iron is at the pore surface, the surface density σ_S of paramagnetic centers is 3.46×10^{11} Fe cm^{-2} for the 75-Å glass and 4.27×10^{11} Fe cm^{-2} for the 159-Å glass. The average distance between the paramagnetic centers is then on the order of $1/\sqrt{\sigma_S}$, which is $\sim$170 Å for the 75-Å glass and $\sim$153 Å in 159-Å glass samples. These figures provide an estimate of the range for the persistence length of the two-dimensional character sensed by the magnetic relaxation of the proton spins induced by the paramagnetic center.

The slopes for the linear portions shown in Figs. 3 and 4 depend on solvent and temperature; however, the ratio of these slopes is indeed 10:3, which is consistent with and supports the theoretical result summarized by Eq. (19). It is important to note that Eq. (19) was derived without an explicit inclusion of the electron-spin relaxation rate as a potential source of important fluctuations in the electron-nuclear coupling. Were the electron-spin relaxation time sufficiently short that it competed with the translational diffusion times, then the low-field portion of the relaxation dispersion would be independent of field strength, which is not consistent with observation. Thus the neglect of the electron-spin relaxation is supported by the experimental result.

In approaching a quantitative test of the relaxation model, the approach is to minimize the number of adjustable parameters. To this end we have used the molecular modeling program INSIGHT2 to fit the different solvent molecules into spheres as an estimate of molecular diameters δ. This procedure gives a δ of 6.12, 6.18, 7.50, and 7.06 Å for acetone, acetonitrile, DMF, and DMSO, respectively. There remain only two adjustable parameters: the distance of minimal approach between the I and S spins δ' and the translational diffusion coefficient $D_{I\perp}$ for the proton-bearing molecule. Although we may adjust δ', its value is constrained by reasonable estimates for the sums of van der Waals radii perhaps modified in the case that a hydrogen bonding interaction is present with OH or FeOH groups at the pore surface.

The solid lines through the data in Figs. 3 and 4 were computed with Eq. (19) as best fits to the data using only δ' and $D_{I\perp}$, as adjustable parameters. The fit to the theory is excellent over the range of magnetic fields studied. The parameters appropriate to 298 K are collected in Table I.

The values of δ', the distance of closest approach, are interesting because they are different for the 75- and the

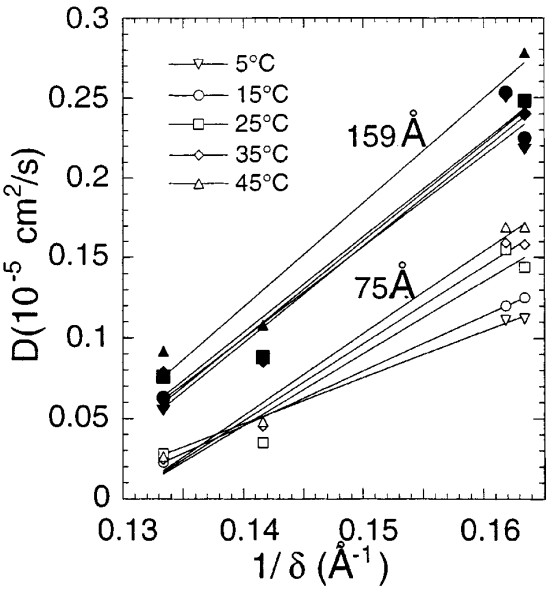

FIG. 5. Translational diffusion coefficient $D_{I\perp}$ as a function of the inverse of the molecular size δ for several temperatures in microporous glass samples of pore sizes 75 and 159 Å. $D_{I\perp}$ is found from the fits of Figs. 3 and 4, with Eq. (19).

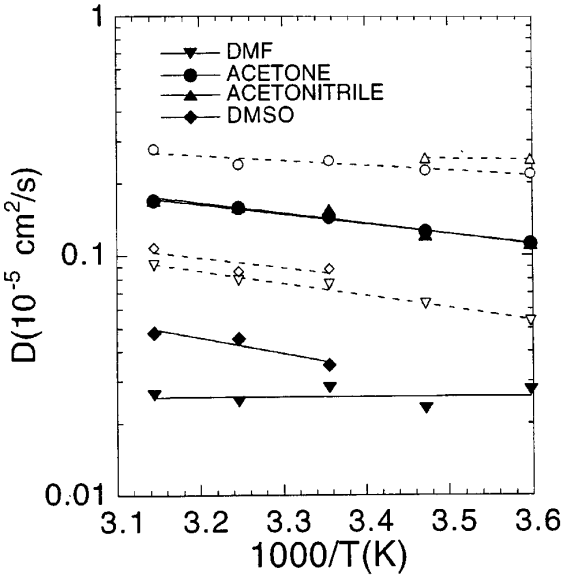

FIG. 6. Semilogarithmic plot of the translational diffusion coefficient $D_{I\perp}$ as a function of the inverse of the temperature for different polar molecules. The filled and open experimental points correspond to glasses of pore sizes 75 and 159 Å, respectively.

159-Å systems. The values for the 75-Å glass are large and represent the kinds of number expected for solvent molecules colliding with a completed first coordination sphere environment for the paramagnetic metal center. Similar values have been obtained for metal complexes in solution [20–22]. However, this parameter is substantially smaller in the case of the 159-Å glass system even though the diffusion coefficients change as expected. This change may result from an effective change in the surface geometry of the solvent or it may derive from an underestimate of the paramagnetic concentration.

The values of the diffusion coefficients obtained by this procedure are about an order of magnitude smaller than values for the bulk solvent, which is consistent with other measurements of surface translational diffusion [23]. Based on the effects of confinement, we expect that the translational diffusion coefficient should increase with increasing pore size [23,24]. Figure 5 shows a plot of the derived diffusion coefficient $D_{I\perp}$ vs $1/\delta$, the inverse of the molecular diameter. The approximately linear dependence of the diffusion constant on the reciprocal of molecular diameter is consistent with Stokes law for the liquid dynamics in the confined spaces of the pores. Further, the temperature dependence is weak. The observed increase of $D_{I\perp}$ with the pore size d (Fig. 5) seems to vary in the same sense as the experimental dependence found by pulsed gradient field method [23]. It is also coherent with some recent mode-coupling theoretical calculations of diffusive motion in confined fluids [24].

The derived translational diffusion constants are plotted vs the reciprocal temperature in Fig. 6 for the four polar liquids and the two porous glasses. In all cases the linear relationships associated with an exponential activation law are obeyed well, although the activation energies associated with these diffusion constants are small and range from 2 to 3 kcal/mol. This verifies that the surface constrained translational reported by the magnetic relaxation dispersion experiment is a thermally activated process.

V. CONCLUSION

A theory of dipolar nuclear-spin relaxation of a polar liquid diffusing in a model pore system in close proximity to highly diluted paramagnetic species fixed at the pore surface is presented. An application of such a theory is proposed to interpret the low-magnetic-field dependence of ^{1}H spin-lattice relaxation of four different aprotic polar liquids in suspension of controlled pore chromatographic glass beads. The unique properties of the magnetic-field dependences of these relaxation rates have allowed a direct measurement of the translational diffusion coefficients of these solvents at the surface of the pores.

ACKNOWLEDGMENTS

The authors gratefully acknowledge useful discussions with Professor J. Freed and Dr. Sandip Sur and the assistance of Dr. L. Henry Bryant. This work was supported in part by the National Institutes of Health, Grant Nos. GM-30309 and GM-34541, and the University of Virginia.

APPENDIX A: CALCULATION OF CORRELATION FUNCTIONS $G_M^{(m')}(\tau)$

The bulk and surface pairwise dipolar correlation functions, in the lamellar frame M, are given from Eqs. (13) and (14) as

$$G_{M,\mathrm{bulk}}^{(m')}(\tau)=\frac{2\pi\sigma_s}{d^2}\int_0^\infty dk\ k\ \exp(-k^2 D_{I\perp}\tau) \times\left|\int_{\delta'}^{d-\delta'} dz\int_0^\infty d\rho\ \rho\ f_2^{(m')}(\rho,z)J_{m'}(k\rho)\right|^2, \tag{A1a}$$

$$G^{(m')}_{M,\mathrm{surface}}(\tau)=\frac{4\pi\sigma_s}{d^2}\int_0^\infty dk\ k\ \exp(-k^2D_{I\perp}\tau)\times\left|\int_0^{\delta'}dz\int_{\delta'}^\infty d\rho\ \rho\ f_2^{(m')}(\rho,z)J_{m'}(k\rho)\right|^2, \tag{A1b}$$

where $J_{m'}(k\rho)$ is an integer Bessel function of integer order m'.

1. Calculation of $G^{(0)}_{M,\mathrm{bulk}}(\tau)$

To calculate $G^{(0)}_{M,\mathrm{bulk}}(\tau)$, one substitutes the value of $f_2^{(0)}$ given in Eq. (4b) into Eq. (A1a) and obtains

$$G^{(0)}_{M,\mathrm{bulk}}(\tau)=\frac{3\pi\sigma_s}{4d^2}\int_0^\infty dk\ k\ \exp(-k^2D_{I\perp}\tau)\times\left|\int_0^\infty d\rho\ \rho\ J_0(k\rho)\int_{\delta'}^{d-\delta'}dz\ \frac{2z^2-\rho^2}{(z^2+\rho^2)^{5/2}}\right|^2. \tag{A2}$$

The integration on z in Eq. (A2) is elementary. We then introduce the two dimensionless variables $y=k\delta'$ and $u=k\rho$ and use the transverse correlation time $\tau_\perp$ given in the text with $\delta'=\delta/2$,

$$G^{(0)}_{M,\mathrm{bulk}}(\tau)=\frac{3\pi\sigma_s}{4d^2\delta'^2}\int_0^\infty dy\ y^3\ e^{-y^2\tau/\tau_\perp}|I_{0,0}(y)|^2,$$

with

$$I_{0,0}(y)=\int_0^\infty du\ u\ J_0(u)\left[\frac{1}{(u^2+y^2)^{3/2}}-\frac{\frac{d}{\delta'}-1}{\left[u^2+y^2\left(\frac{d}{\delta'}-1\right)^2\right]^{3/2}}\right]=\frac{1}{y}\left[e^{-y}-e^{-y(d/\delta'-1)}\right]. \tag{A3}$$

As described in the text and because of the exponential factor $\exp(-y^2\tau/\tau_\perp)$, the dominant term at long time (when $\tau\gg\tau_\perp$) of Eq. (A3) comes only from the long wavelength, $y\to0$, transverse diffusion mode. This allows a simplification of $I_{0,0}(y)$, which becomes $I_{0,0}(y)\sim(d/\delta'-2)+O(y)$ or simply $d/\delta'+O(y)$ when $d/\delta'\gg1$. Then the leading term of $G^{(0)}_{M,\mathrm{bulk}}(\tau)$ when $\tau\gg\tau_\perp$ is given by the power law

$$G^{(0)}_{M,\mathrm{bulk}}(\tau)=\frac{3\pi\sigma_s}{4\delta'^4}\int_0^\infty dy\ y^3e^{-y^2\tau/\tau_\perp}=\frac{3\pi\sigma_s}{8\delta'^4}\left(\frac{\tau_\perp}{\tau}\right)^2. \tag{A4}$$

2. Calculation of $G^{(0)}_{M,\mathrm{surface}}(\tau)$

Using the same procedure, one obtains the expression for $G^{(0)}_{M,\mathrm{surface}}(\tau)$,

$$G^{(0)}_{M,\mathrm{surface}}(\tau)=\frac{3\pi\sigma_s}{2d^2\delta'^2}\int_0^\infty dy\ y^3e^{-y^2\tau/\tau_\perp}|I_{0,1}(y)|^2,$$

with

$$I_{0,1}(y)=\int_y^\infty du\ u\ \frac{J_0(u)}{(u^2+y^2)^{3/2}}=\int_0^\infty du\ u\ \frac{J_0(u)}{(u^2+y^2)^{3/2}}-\int_0^y du\ u\ \frac{J_0(u)}{(u^2+y^2)^{3/2}}=\frac{1}{\sqrt{2}y}-1+\frac{3}{4\sqrt{2}}y-\frac{1}{6}y^2+O(y^3). \tag{A5}$$

Then the leading term of $G^{(0)}_{M,\mathrm{surface}}(\tau)$, when $\tau\gg\tau_\perp$, is given by

$$G^{(0)}_{M,\mathrm{surface}}(\tau)=\frac{3\pi\sigma_s}{2d^2\delta'^2}\int_0^\infty dy\ y\ e^{-y^2\tau/\tau_\perp}\left[\frac{1}{2}-\sqrt{2}y+\frac{7}{4}y^2\right]=\frac{3\pi\sigma_s}{2d^2\delta'^2}\left[\frac{1}{4}\left(\frac{\tau_\perp}{\tau}\right)-\frac{1}{4}\left(\frac{\tau_\perp}{\tau}\right)^{3/2}+\frac{7}{8}\left(\frac{\tau_\perp}{\tau}\right)^2\right]\approx\frac{3\pi\sigma_s}{8d^2\delta'^2}\left(\frac{\tau_\perp}{\tau}\right). \tag{A6}$$

3. Calculations of $G^{(m)}_{M,\mathrm{bulk}}(\tau)$ and $G^{(m)}_{M,\mathrm{surface}}(\tau)$ for $m=1$ and 2

Calculations similar to those given above lead to the following power laws valid when $\tau\gg\tau_\perp$:

$$G^{(1)}_{M,\mathrm{bulk}}(\tau)=G^{(-1)}_{M,\mathrm{bulk}}(\tau)=\frac{\pi\sigma_s}{4\delta'^4}\left(\frac{\tau_\perp}{\tau}\right)^2, \tag{A7a}$$

$$G^{(1)}_{M,\mathrm{surface}}(\tau)=G^{(-1)}_{M,\mathrm{surface}}(\tau)=\frac{\pi\sigma_s}{8d^2\delta'^2}\left(\frac{3}{\sqrt{2}}-1\right)^2\left(\frac{\tau_\perp}{\tau}\right)^2 \tag{A7b}$$

and

$$G^{(2)}_{M,\mathrm{bulk}}(\tau)=G^{(2)}_{M,\mathrm{bulk}}(\tau)=\frac{\pi\sigma_s}{16\delta'^4}\left(\frac{\tau_\perp}{\tau}\right)^2, \tag{A8a}$$

$$G^{(2)}_{M,\mathrm{surface}}(\tau)=G^{(-2)}_{M,\mathrm{surface}}(\tau)=\frac{\pi\sigma_s}{8d^2\delta'^2}\left(\frac{\tau_\perp}{\tau}\right)^2. \tag{A8b}$$

APPENDIX B: CALCULATION OF SPECTRAL DENSITIES $J^{(m')}_M(\omega)$

1. Calculation of $J^{(0)}_{M,\mathrm{bulk}}(\tau)$

The spectral density $J^{(0)}_{M,\mathrm{bulk}}(\omega)$ is obtained by the exponential Fourier transform of Eq. (A3),

$$J^{(0)}_{M,\mathrm{bulk}}(\omega)=\frac{3\pi\sigma_s}{4d^2\delta'^2}\,2\tau_\perp\int_0^\infty dy\,\frac{y^3}{y^4+\omega^2\tau_\perp^2}\times\left[e^{-y}-e^{-y(d/\delta'-1)}\right]^2. \tag{B1}$$

We introduce the new variable x defined by $y=x\sqrt{\omega\tau_\perp}$ and Eq. (B1) becomes

$$J^{(0)}_{M,\mathrm{bulk}}(\omega)=\frac{3\pi\sigma_s}{4d^2\delta'^2}\,2\tau_\perp\int_0^\infty dx\,\frac{x^3}{x^4+1}\left[e^{-x\sqrt{\omega\tau_\perp}}-e^{-x\sqrt{\omega\tau_\perp}(d/\delta'-1)}\right]^2, \tag{B2}$$

where one expands the integrand in rational functions of lower degree

$$J^{(0)}_{M,\mathrm{bulk}}(\omega)=\frac{6\pi\sigma_s}{4d^2\delta'^2}\,\tau_\perp\int_0^\infty dx\,\frac{x}{4\sqrt{2}}\left\{(1+i)\left[\frac{1}{x-x_1^*}-\frac{1}{x+x_1^*}\right]+(1+i)\left[\frac{1}{x-x_1}-\frac{1}{x+x_1}\right]\right\}\times\left[e^{-x\sqrt{\omega\tau_\perp}}-e^{-x\sqrt{\omega\tau_\perp}(d/\delta'-1)}\right]^2, \tag{B3}$$

where $x_1=e^{i\pi/4}$ and x_1^* is its complex conjugate. Each of the integrals in Eq. (B3) can be expressed in terms of the exponential integral function $E_1(z)$,

$$E_1(z)=\int_z^\infty\frac{e^{-u}}{u}\,du\approx-\gamma-\ln(z)-\sum_{n=1}^{\infty}(-1)^n\frac{z^n}{nn!}, \tag{B4}$$

where γ is the Euler constant. After some straightforward calculations, one has

$$\begin{aligned}J^{(0)}_{M,\mathrm{bulk}}(\omega)=\frac{3\pi\sigma_s}{4d^2\delta'^2}\,\tau_\perp\,\mathrm{Re}\Big\{&e^{2x_1\sqrt{\omega\tau_\perp}}E_1(2x_1\sqrt{\omega\tau_\perp})\\&+e^{-2x_1\sqrt{\omega\tau_\perp}}E_1(-2x_1\sqrt{\omega\tau_\perp})\\&+e^{2x_1(d/\delta'-1)\sqrt{\omega\tau_\perp}}E_1\left[2x_1\left(\frac{d}{\delta'}-1\right)\sqrt{\omega\tau_\perp}\right]\\&+e^{-2x_1(d/\delta'-1)\sqrt{\omega\tau_\perp}}E_1\left[-2x_1\left(\frac{d}{\delta'}-1\right)\sqrt{\omega\tau_\perp}\right]\\&-2\left[e^{x_1(d/\delta')\sqrt{\omega\tau_\perp}}E_1\left(x_1\,\frac{d}{\delta'}\,\sqrt{\omega\tau_\perp}\right)\right.\\&\left.+e^{-x_1(d/\delta')\sqrt{\omega\tau_\perp}}E_1\left(-x_1\,\frac{d}{\delta'}\,\sqrt{\omega\tau_\perp}\right)\right]\Big\}.\end{aligned} \tag{B5}$$

This expression becomes constant at low frequency when $\omega\tau_\perp\ll1$,

$$J^{(0)}_{M,\mathrm{bulk}}(\tau)=\frac{3\pi\sigma_s}{2d^2\delta'^2}\,\tau_\perp\left\{\ln\left(\frac{d}{\delta'}+1\right)-2\ln 2+O(\sqrt{\omega\tau_\perp})\right\}. \tag{B6}$$

2. Calculation of $J^{(0)}_{M,\mathrm{surface}}(\tau)$

The spectral density $J^{(0)}_{M,\mathrm{surface}}(\omega)$ is obtained by the exponential Fourier transform of Eq. (A6),

$$J^{(0)}_{M,\mathrm{surface}}(\omega)=\frac{3\pi\sigma_s\tau_\perp}{d^2\delta'^2}\int_0^\infty dy\,\frac{y^3}{y^4+\omega^2\tau_\perp^2}\left[\frac{1}{2}-\sqrt{2}y+\frac{7}{4}y^2-\frac{11}{6\sqrt{2}}y^3+\cdots\right]. \tag{B7}$$

We introduce the same dimensionless variable x defined in Eq. (B2),

$$J^{(0)}_{M,\mathrm{surface}}(\omega)=\frac{3\pi\sigma_s\tau_\perp}{d^2\delta'^2}\int_0^{1/\sqrt{\omega\tau_\perp}}dx\,\frac{x^3}{x^4+1}\left[\frac{1}{2}-\sqrt{2}x\sqrt{\omega\tau_\perp}+\frac{7}{4}x^2\omega\tau_\perp-\frac{11}{6\sqrt{2}}x^3(\omega\tau_\perp)^{3/2}+\cdots\right]. \tag{B8}$$

Here we have limited the domain of integration to the range of long wavelength ($y\to0$); this ensures the convergence of the integral without changing the leading term when $\omega\tau_\perp\ll1$,

$$J^{(0)}_{M,\mathrm{surface}}(\omega)=\frac{3\pi\sigma_s\tau_\perp}{d^2\delta'^2}\left[-0.846+\frac{1}{8}\ln\left(1+\frac{1}{\omega^2\tau_\perp^2}\right)+O(\sqrt{\omega\tau_\perp})\right]. \tag{B9}$$

3. Calculations of $J^{(m)}_{M,\mathrm{bulk}}(\tau)$ and $J^{(m)}_{M,\mathrm{surface}}(\tau)$ for $m=1$ and 2

Calculations similar to those given above lead to the following spectral densities when $\omega\tau_\perp\ll1$:

$$J^{(1)}_{M,\mathrm{bulk}}(\omega)=J^{(-1)}_{M,\mathrm{bulk}}(\omega)=\frac{\pi\sigma_s\tau_\perp}{d^2\delta'^2}\left[\ln\left(\frac{d}{\delta'}+1\right)-2\ln 2+O(\sqrt{\omega\tau_\perp})\right], \tag{B10a}$$

$$J^{(1)}_{M,\mathrm{surface}}(\omega)=J^{(-1)}_{M,\mathrm{surface}}(\omega)=\frac{2\pi\sigma_s\tau_\perp}{d^2\delta'^2}\left[0.049-O(\sqrt{\omega\tau_\perp})\right] \tag{B10b}$$

and

$$J^{(2)}_{M,\mathrm{bulk}}(\omega)=J^{(-2)}_{M,\mathrm{bulk}}(\omega)=\frac{\pi\sigma_s\tau_\perp}{4d^2\delta'^2}\left[\ln\left(\frac{d}{\delta'}+1\right)-2\ln 2+O(\sqrt{\omega\tau_\perp})\right], \tag{B10c}$$

$$J^{(2)}_{M,\mathrm{surface}}(\omega)=J^{(-2)}_{M,\mathrm{surface}}(\omega)=\frac{\pi\sigma_s\tau_\perp}{2d^2\delta'^2}\left[0.226-O(\sqrt{\omega\tau_\perp})\right]. \tag{B10d}$$

APPENDIX C: CALCULATION OF THE POWDER AVERAGE OF MAGNETIZATION

The experiments described in the text require that each micropore at angle β will relax exponentially with its own spin-lattice relaxation rate $1/T_1(\beta)$. The observed longitudinal magnetization $\langle M_z(t)\rangle$ then becomes

$$\langle M_z(t)\rangle = M_{\rm eq}\left[1-2\left\langle \exp\left(-\frac{1}{T_1(\beta)}\right)\right\rangle\right], \tag{C1}$$

where the thermal equilibrium magnetization is $M_{\rm eq}$ and the average over the Euler angles is given by

$$\left\langle \exp\left(-\frac{t}{T_1(\beta)}\right)\right\rangle = \frac{1}{2}\int_0^{2\pi} \exp\left(-\frac{t}{T_1(\beta)}\right)\sin\beta\, d\beta. \tag{C2}$$

It is well known [25] that Eq. (C2) can be written as

$$\left\langle \exp\left(-\frac{t}{T_1(\beta)}\right)\right\rangle = \exp\left[-\left\langle\frac{1}{T_1(\beta)}\right\rangle t+\sum_{n=2}^{\infty}\frac{(-1)^n}{n!}\,t^n C_n\right], \tag{C3}$$

where C_n are the so-called cumulants that represents the deviations from a single exponential decay.

As the observed relaxation decays are exponential, to within our precision ($\sim 3\%$), it is legitimate to limit the infinite expansion of Eq. (C3) to the first three cumulants

$$C_1=\left\langle\frac{1}{T_1(\beta)}\right\rangle,$$

$$C_2=\left\langle\left(\frac{1}{T_1(\beta)}\right)^2\right\rangle-\left\langle\frac{1}{T_1(\beta)}\right\rangle^2, \tag{C4}$$

$$C_3=\left\langle\left(\frac{1}{T_1(\beta)}\right)^3\right\rangle-3\left\langle\left(\frac{1}{T_1(\beta)}\right)^2\right\rangle\left\langle\frac{1}{T_1(\beta)}\right\rangle+2\left\langle\frac{1}{T_1(\beta)}\right\rangle^3.$$

The deviation from the single exponential may be estimated through the coefficent $\Delta(t)$ [25],

$$\Delta(t)=\frac{\left\langle\exp\left(-\frac{t}{T_1(\beta)}\right)\right\rangle}{\exp\left[-\left\langle\frac{1}{T_1(\beta)}\right\rangle t\right]}-1\sim\exp\left[\frac{1}{2}\,C_2t^2-\frac{1}{6}\,C_3t^3\right]-1. \tag{C5}$$

Using the spectral densities coming from Eqs. (17)

$$J_L^{(0)}(\omega)\approx|d^{(2)}_{0,0}(\beta)|^2J_M^{(0)}(\omega),$$

$$J_L^{(1)}(\omega)\approx|d^{(2)}_{1,0}(\beta)|^2J_M^{(0)}(\omega), \tag{C6}$$

$$J_L^{(2)}(\omega)\approx|d^{(2)}_{2,0}(\beta)|^2J_M^{(0)}(\omega),$$

one obtains the expressions of the first three cumulants [Eqs. (C4)], after some straightforward calculations one has

$$\begin{aligned}\Delta(t)=\exp\Bigg\{&\frac{t^2}{3150}\left[27J_M^{(0)}(\omega_1)^2-84J_M^{(0)}(\omega_1)J_M^{(0)}(\omega_S)\right.\\&\left.+92J_M^{(0)}(\omega_S)^2\right]-\frac{t^3}{10\,135\,125}\left[513J_M^{(0)}(\omega_1)^3\right.\\&-3294J_M^{(0)}(\omega_1)^2J_M^{(0)}(\omega_S)+11\,484J_M^{(0)}(\omega_1)J_M^{(0)}(\omega_S)^2\\&\left.-5128J_M^{(0)}(\omega_S)^3\right]\Bigg\}-1.\end{aligned} \tag{C7}$$

For values of t ranging between 0 and $1/C_1$, $\Delta(t)$ stays very small, for instance, $\Delta(1/C_1)\leqslant 0.01$. As a consequence, there is no observable deviation from the single exponential; we consider in the paper the approximation

$$\begin{aligned}\left\langle\exp\left(-\frac{t}{T_1(\beta)}\right)\right\rangle&\approx\exp\left[-\left\langle\frac{1}{T_1(\beta)}\right\rangle t+\frac{1}{2}\,C_2t^2-\frac{1}{6}\,C_3t^3\right]\\&\approx\exp\left[-\left\langle\frac{1}{T_1(\beta)}\right\rangle t\right],\end{aligned} \tag{C8}$$

which has been used in Eqs. (17)–(19).

[1] D. P. Gallegos, D. M. Smith, and C. J. Brinker, J. Colloid Interface Sci. **124**, 186 (1988).

[2] F. d'Orazio, S. Bhattacharja, W. Halperin, and R. Gerhardt, Phys. Rev. Lett. **63**, 43 (1989); J. Y. Jehng, Ph.D. thesis, Northwestern University, 1995 (unpublished).

[3] G. Liu, Y. Li, and J. Jonas, J. Chem. Phys. **95**, 6892 (1991).

[4] J.-P. Korb, Shu Xu, and J. Jonas, J. Chem. Phys. **98**, 2411 (1993).

[5] J.-P. Korb, A. Delville, Shu Xu, G. Demeulenaere, G. Costa, and J. Jonas, J. Chem. Phys. **101**, 7074 (1994).

[6] R. Kimmich and H. W. Weber, Phys. Rev. B **47**, 11 788 (1993).

[7] J.-P. Korb, L. Malier, F. Cros, Shu Xu, and J. Jonas, Phys. Rev. Lett. **77**, 2312 (1996).

[8] S. Stapf and R. Kimmich, J. Chem. Phys. **103**, 2247 (1995).

[9] M. Whaley, Alexia J. Lawrence, Jean-Pierre Korb, and R. G. Bryant, Solid State Nucl. Magn. Reson. **7**, 247 (1996).

[10] F. Noack, Bull. Ampere **175**, 18 (1994).

[11] A. Abragam, *The Principles of Nuclear Magnetism* (Clarendon, Oxford, 1961), Chap. VIII.

[12] D. A. Varshalovich, A. N. Moskalev, and V. K. Khersonskii, *Quantum Theory of Angular Momentum* (World Scientific, Singapore, 1988), Chap. 4.

[13] H. S. Carslaw and J. C. Jaeger, *Conduction of Heat in Solids* (Clarendon, Oxford, 1959).

[14] Y. Ayant, E. Belorizky, J. Alizon, and J. Gallice, J. Phys. (France) **36**, 991 (1975).

[15] J.-P. Korb, D. C. Torney, and H. M. McConnell, J. Chem. Phys. **78**, 5782 (1983); J.-P. Korb, M. Winterhalter, and H. M. McConnell, *ibid.* **80**, 1059 (1984); J. Tabony and J.-P. Korb, Mol. Phys. **56**, 1281 (1985); J.-P. Korb, M. Ahadi, G. P. Zientara, and J. Freed, J. Chem. Phys. **86**, 1125 (1987).

[16] I. Solomon, Phys. Rev. **99**, 559 (1955); N. Bloembergen and L. O. Morgan, J. Chem. Phys. **34**, 842 (1961).
[17] A. G. Redfield, W. Fite, and H. E. Bleich, Rev. Sci. Instrum. **39**, 710 (1968).
[18] S. H. Koenig and W. E. Schillinger, J. Biol. Chem. **12**, 3283 (1969).
[19] G. Hernandez, M. F. Tweedle, H. Brittain, and R. G. Bryant, Inorg. Chem. **29**, 985 (1990).
[20] C. C. Lester and R. G. Bryant, J. Phys. Chem. **94**, 2843 (1990).
[21] C. F. Polnaszek and R. G. Bryant, J. Am. Chem. Soc. **106**, 428 (1984).
[22] C. F. Polnaszek, D. Hanggi, P. W. Carr and R. G. Bryant, Anal. Chem. Acta **194**, 311 (1987).
[23] A. Mitzithras and J. H. Strange, Magn. Reson. Imaging **12**, 261 (1994).
[24] L. Bocquet and J. L. Barrat, Europhys. Lett. **31**, 455 (1995).
[25] J. Peternelj and M. Pintar, Phys. Rev. B **15**, 5097 (1977).